Kinetic Mechanism of Nicotinic Acid Phosphoribosyltransferase: Implications for Energy Coupling†

Jeffrey W. Gross, Mathumathi Rajavel,‡ and Charles Grubmeyer*

Department of Biochemistry and Fels Institute for Cancer Research and Molecular Biology, Temple University School of Medicine, 3307 North Broad Street, Philadelphia, Pennsylvania 19140

Received August 13, 1997

ABSTRACT: Nicotinic acid phosphoribosyltransferase (NAPRTase; EC 2.4.2.11) is a facultative ATPase that uses the energy of ATP hydrolysis to drive the synthesis of nicotinate mononucleotide and pyrophosphate from nicotinic acid (NA) and phosphoribosyl pyrophosphate (PRPP). To learn how NAPRTase uses this hydrolytic energy, we have further delineated the kinetic mechanism using steady-state and pre-steady-state kinetics, equilibrium binding, and isotope trapping. NAPRTase undergoes covalent phosphorylation by bound ATP at a rate of 30 s^{-1}. The phosphoenzyme (E−P) binds PRPP with a K_D of 0.6 μM, a value 2000-fold lower than that measured for the nonphosphorylated enzyme. The minimal rate constant for PRPP binding to E−P is 0.72×10^5 M^{-1} s^{-1}. Isotope trapping shows that greater than 90% of bound PRPP partitions toward product upon addition of NA. Binding of NA to E−P·PRPP is rapid, $k_{on} \geq 7.0 \times 10^6$ M^{-1} s^{-1}, and is followed by rapid formation of NAMN and PP_i, $k \geq 500$ s^{-1}. After product formation, E−P undergoes hydrolytic cleavage, $k = 6.3$ s^{-1}, and products NAMN, PP_i, and P_i are released. Quenching from the steady state under V_{max} conditions indicates that slightly less than half the enzyme is in phosphorylated forms. To account for this finding, we propose that one step in the release of products is as slow as 5.2 s^{-1} and, together with the E−P cleavage step, codetermines the overall k_{cat} of 2.3 s^{-1} at 22 °C. Energy coupling by NAPRTase involves two strategies frequently proposed for ATPases of macromolecular recognition and processing. First, E−P has a 10^3-fold higher affinity for substrates than does nonphosphorylated enzyme, allowing the E−P to bind substrate from low concentration and nonphosphorylated enzyme to expel products against a high concentration. Second, the kinetic pathway follows "rules" [Jencks, W. P. (1989) *J. Biol. Chem. 264*, 18855−18858] that minimize unproductive alternative reaction pathways. However, an analysis of reaction schemes based on these strategies suggests that such nonvectorial reactions are intrinsically inefficient in ATP use.

NAPRTase[1] (EC 2.4.2.11) presents an interesting case in which enzymic intermediates couple ATP hydrolysis and nucleotide formation. The *Salmonella typhimurium* enzyme is a facultative ATPase, using ATP hydrolysis to accelerate and provide a thermodynamic drive for the reaction:

$$PRPP + NA \rightleftharpoons NAMN + PP_i$$

The enzyme catalyzes NAMN formation without ATP, but the reaction is accelerated 10−30-fold in its presence. With the hydrolysis of ATP, the enzyme can produce and sustain an approximate 10^3-fold increase in the ratio [NAMN][PP_i]/[PRPP][NA] from its equilibrium value of 0.67 (*1*). Among enzymes that couple conversions of metabolic intermediates to the hydrolysis of ATP, NAPRTase has several features that are unusual. First, ATP is used to phosphorylate the enzyme. No phosphorylated substrate derivatives occur along the reaction pathway. Second, the increased products/substrates ratio is a transient, steady-state phenomenon, collapsing to the equilibrium value when the supply of ATP is exhausted. Third, the enzyme is inefficient in capturing the energy of ATP hydrolysis, attaining only about 0.1% of the product/substrate ratio of about 10^6 that should result from coupled ATP cleavage. Finally, the kinetic scheme for NAPRTase is branched, allowing for at least two competing reactions. The enzyme catalyzes ATP hydrolysis, induced by PP_i in solution, as well as NAMN synthesis and pyrophosphorolysis in the absence of ATP or ADP and P_i. These properties of NAPRTase are more characteristic of the enzymes that use ATP hydrolysis in macromolecular recognition and processing (*2*). Consequently, NAPRTase may serve as an easily studied paradigm for those more complex systems.

We have analyzed the catalytic and alternative reactions of NAPRTase in terms of Scheme 1, which was proposed on the basis of steady-state kinetics, isotope exchange, and phosphorylation experiments (*1*, *3*−*5*). Scheme 1 represents

† This research was supported by a grant from the National Science Foundation (DMB91-03029). J.G. is the recipient of federal work study funds.

* To whom correspondence should be addressed: Phone 215-707-4495; FAX 215-707-7536; email ctg@ariel.fels.temple.edu.

‡ Present address: Department of Biochemistry, Johns Hopkins University, 615 N. Wolfe St., Baltimore, MD 21205.

[1] Abbreviations: WT, wild-type enzyme; NA, nicotinic acid; NAMN, nicotinic acid mononucleotide; NAPRTase, nicotinic acid phosphoribosyltransferase; PRPP, α-D-5-phosphoribosyl 1-pyrophosphate; PP_i, pyrophosphate; AMP-PCP, β,γ-methyleneadenosine 5′-triphosphate; DTT, dithiothreitol; PEP, phosphoenolpyruvate; HGPRTase, hypoxanthine−guanine phosphoribosyltransferase; OPRTase, orotate phosphoribosyltransferase.

S0006-2960(97)02014-X CCC: $15.00
Published on Web 03/06/1998

Scheme 1

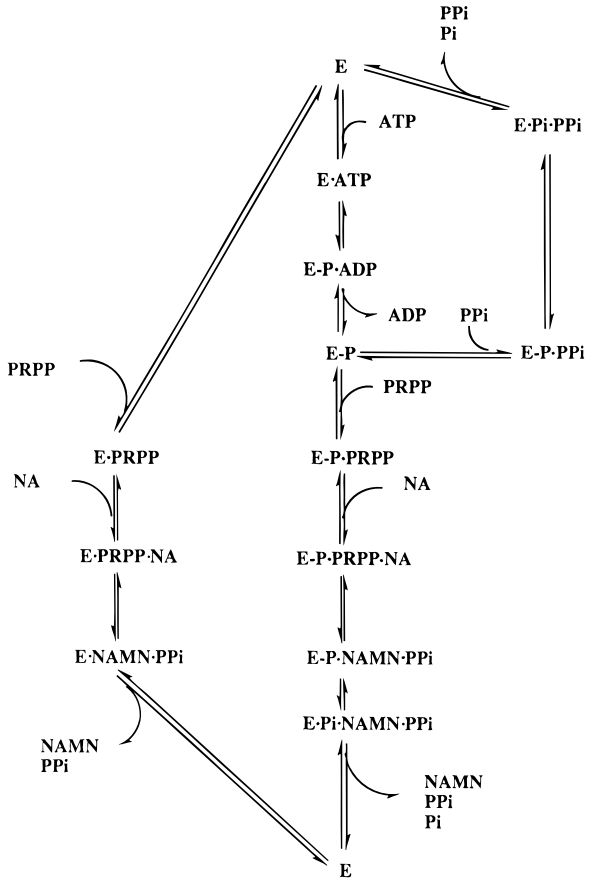

a branched pathway with the ATP-coupled reaction shown as the central path. The uncoupled NAMN synthesis and the product-stimulated ATPase reactions are shown, respectively, to the left and right of the coupled reaction. The scheme proposes an alternation of enzyme forms (E and E−P) that differ in their enzymic properties and link the ATPase reaction with NAMN synthesis. From K_M and k_{cat} values, the nonphosphorylated E form of NAPRTase is proposed to be a poor catalyst, with weak binding of substrates and a poor catalytic rate. In contrast, the E−P arising from phosphorylation at His-219 has been shown to have 200-fold lower K_M values than E and a k_{cat} value that is 10−30-fold higher. Our knowledge of the exact events of coupled NAMN formation is more speculative. The scheme proposes the compulsory hydrolysis of E−P after conversion of enzyme-bound NA and PRPP to bound NAMN and PP_i. The E·P_i·NAMN·PP_i complex, which is presumed to share the low-affinity properties of E rather than the high affinity of E−P, must then dissociate to release products P_i, PP_i, and NAMN. By using ATP to ensure rapid conversion of free E to E−P, a cycle is created in which substrates are captured, converted to products, and driven off the active site, allowing for a displacement of the [NAMN][PP_i]/[PRPP]-[NA] ratio from its equilibrium value.

The scheme is speculative in several respects. First among these is the order of events. To capture the energy of E−P hydrolysis effectively, NAMN and PP_i formation are placed before E−P cleavage, but no direct evidence for this exists. Second, although K_M and k_{cat} values support a dramatic difference between E and E−P, no direct measurements of binding affinities or rate constants for individual steps have been made. Finally, the scheme proposes that the interconversion of enzyme forms is triggered by a reaction intermediate. Is the compulsory decomposition of E−P·NAMN·PP_i to E·P_i·NAMN·PP_i, followed by product release, sufficient to capture the complete energy of ATP hydrolysis in the form of a [NAMN][PP_i]/[PRPP][NA] gradient? Here we have used binding, isotope trapping, and steady-state and pre-steady-state kinetics to address these issues. We define rate constants for many of the reaction steps of Scheme 1 and use the constants to reconsider the effiency of energy coupling by NAPRTase. We find that inefficency is intrinsic to the reaction cycle itself, a finding with implications for other ATPases of macromolecular recognition and processing.

EXPERIMENTAL PROCEDURES

Materials. [β-^{32}P]PRPP was synthesized as described by Xu et al. (*6*). [γ-^{32}P]ITP was synthesized as described by Grubmeyer and Penefsky (*7*). [γ-^{32}P]ATP (3 Ci/mmol) was obtained from Amersham, $^{32}P_i$, [^{32}P]PP_i, and [^{14}C]NA were from NEN−DuPont. Pyruvate kinase, lactate dehydrogenase, and inorganic pyrophosphatase were from Boehringer Mannheim; Sephadex G50 was from Pharmacia. HPLC solvents and other chemicals were from Fisher. Poly(ethylenimine)−cellulose plates (Polygram CEL 300 PEI; Macherey-Nagel Inc.) were from Alltech, Deerfield, IL. All other biochemicals were from Sigma. *S. typhimurium* NAPRTase was purified as previously described (*2*). The enzyme was homogeneous as judged by SDS−PAGE with Coomassie blue staining.

Quantitative amino acid analysis was performed at the Wistar Protein Microchemistry Facility. In three separate analyses, duplicate samples were hydrolyzed with 6 N HCl and 1% phenol for 1 h at 160 °C in vapor phase, followed by manual PTC derivatization and HPLC separation (*8*). The experimentally determined E_{280nm} for a 1 mg/mL solution, 1.65, was 1.3-fold higher than the calculated value of 1.27 (*9*), and was used in conjunction with the M_r of 45 529 to calculate molarity of the monomeric enzyme.

A unit of enzymatic activity is defined as the amount required to catalyze the conversion of 1 μmol of substrate (ATP, NA, or PRPP) to product/min under the stated conditions. Unless otherwise stated, the rates reported here were obtained at room temperature (22−24 °C).

Analysis of Data. Results from steady-state experiments were fit with the programs HYPER and COMPO (*10*) and presented with the standard error. Data from single-turnover experiments were fit with a linear least-squares regression.

Chemical Quench Experiments. Pre-steady-state and single-turnover experiments using chemical quench techniques utilized a Precision Syringe Ram, model 1010 (Update Instruments Inc., Madison, WI). Samples from each of two syringes were injected through a mixing chamber and an aging hose, with 100 μL of the reaction mixture ejected through a nozzle into 500 μL of quench solution (1.2 M NaOH for E−P determination, 6% perchloric acid in all other cases).

Product Purification. For the isolation of [^{14}C]NAMN formed from [^{14}C]NA during chemical quench experiments, quenched samples were neutralized to a pH of approximately 7 with 6 M KOH, incubated on ice for 15 min, and then

centrifuged for 10 min at 14000*g* to remove potassium perchlorate and precipitated protein. Aliquots (100 μL) were injected onto a μBondapak C18 column (3.9 × 300 mm) equilibrated in 10 mM $KHPO_4$, and 0.45 mM tetrabutylammonium dihydrogen phosphate, pH 2.7, and eluted with a 5 mL linear gradient to 100 mM $KHPO_4$ in the same buffer. A flow rate of 1 mL/min was employed. NA elutes 3.8 mL after initiation of the gradient, and NAMN at 8.5 mL. This purification protocol was discontinued due to irreversible loss of column resolution. Subsequently, separation of [^{14}C]-NAMN from [^{14}C]NA was performed using a μBondapak C18 column (3.9 × 300 mm) equilibrated and eluted isocratically in 100 mM sodium acetate, pH 4.5. [^{14}C]-NAMN elutes at 4.5 mL and [^{14}C]NA at 6.5 mL.

ATP Binding and Phosphorylation. To determine the K_I for ATP, 200 μL reactions were incubated at 30 °C and contained 0.21−2.1 mM [γ-^{32}P]ITP, 0−3.0 mM ATP, 0.5 mM PRPP, 0.5 mM NA, 7 mM $MgSO_4$, and 2−20 μg of NAPRTase in buffer N (200 mM monopotassium glutamate and 20 mM Tris-SO_4, pH 8.3) supplemented with 5 mM DTT. Five samples were collected at 1-min intervals. The samples were quenched by injecting 20 μL portions of the reaction into 880 μL of 6% perchloric acid. A 100 μL aliquot of an activated charcoal slurry (8 g/100 mL of H_2O) was added to the quenched samples to adsorb [γ-^{32}P]ITP. Samples were vigorously mixed, incubated for 5 min at 0 °C, and then centrifuged for 10 min at 14000*g*. $^{32}P_i$ in 500 μL of the supernatant was determined by Cerenkov radiation.

Protocols for the formation and isolation of E−P (*5*) were adapted as follows for chemical quench experiments. Syringe A contained 130−175 μM (6−8 mg/mL) NAPRTase in buffer N supplemented with 5 mM DTT. Syringe B contained 0.2−20 mM [γ-^{32}P]ATP (500−2000 cpm/nmol), 3 mM PEP, and 0.15 mg/mL pyruvate kinase in buffer N supplemented with 5 mM DTT. Mg^{2+} was maintained at a minimum 3 mM excess over ATP in all experiments. Reactions were quenched in 1 M NaOH as described above. Protein was separated from noncovalently bound substrates using a centrifuge column method (*11*), in which portions (400 μL) of the quenched reactions were loaded onto 5 mL disposable syringes packed with Sephadex G50 and pre-equilibrated with 6 M urea in 50 mM $KHPO_4$, pH 7.4. Column effluents were diluted with the equilibration buffer to 1 mL. Radioactivity was determined by Cerenkov radiation and protein by A_{280} absorbance.

The level of phosphorylation during steady-state turnover was determined in chemical quench experiments in which syringe A contained 154 μM NAPRTase and 3 mM $MgSO_4$ in buffer N supplemented with 5 mM DTT. Syringe B contained 6 mM [γ-^{32}P]ATP (2000 cpm/nmol), 2 mM PRPP, and 11 mM $MgSO_4$ in buffer N supplemented with 5 mM DTT. The stoichiometry of enzyme phosphorylation in the E-^{32}P·PRPP binary complex at the indicated times of reaction was assayed as described above. Syringe B was then supplemented with 2 mM NA, and the stoichiometry of phosphorylation was assayed at the same times.

Phosphoribosyl Transfer. The rate of phosphoribosyl transfer from the preformed E−P·PRPP binary complex was determined in chemical quench experiments, in which syringe A contained 83 μM NAPRTase, 4.0 mM ATP, 2.0 mM PRPP, 16 mM $MgSO_4$, and 1 unit/mL yeast inorganic pyrophosphatase in buffer N supplemented with 5 mM DTT. Syringe B contained 600 μM [^{14}C]NA in buffer N supplemented with 5 mM DTT. Reactions were quenched in 6% perchloric acid. Separation of [^{14}C]NAMN from [^{14}C]NA was done on the HPLC using the ion pairing method described above.

The rate of phosphoribosyl transfer starting from unliganded NAPRTase was determined in chemical quench experiments in which syringe A contained 0.2 mM [^{14}C]-NA, 2.0 mM PRPP, 20 mM ATP, and 25 mM $MgSO_4$ in buffer N supplemented with 5 mM DTT, and syringe B contained 20 μM NAPRTase and 5 mM $MgSO_4$ in buffer N supplemented with 5 mM DTT. Separation of [^{14}C]NAMN from [^{14}C]NA was performed by HPLC with the sodium acetate buffer.

Substrate Binding to E−P. The apparent k_{on} for NA was determined by mixing substoichiometric quantities of NA with NAPRTase and high levels of ATP and PRPP in single-turnover, chemical quench experiments. Syringe A contained 11−51 μM NAPRTase, 2.0 mM PRPP, 4.0 mM ATP, and 11 mM $MgCl_2$ in buffer N supplemented with 1 mM DTT. Syringe B contained 1.3−6.0 μM [^{14}C]NA in buffer N supplemented with 1 mM DTT. Product separation was done by HPLC with the sodium acetate buffer.

The apparent k_{on} for PRPP was determined in a single-turnover, chemical quench experiment in which syringe A contained 17.6−68.3 μM NAPRTase, 4.0 mM ATP, 0.67 mg/mL pyruvate kinase, 5.0 mM PEP, and 9.0 mM $MgCl_2$ in buffer N supplemented with 1.0 mM DTT. Syringe B contained 0.67−2.0 μM [β-^{32}P]PRPP, 2.0 mM NA, and 5.0 mM $MgCl_2$ in buffer N supplemented with 1.0 mM DTT. Reactions were quenched in 3 M formic acid. Samples (10 μL) were applied to PEI thin-layer chromatography plates and developed with 0.85 M $NaHPO_4$, pH 3.4 (*12*). The TLC plates were exposed to Fuji phosphorimager screens for 16 h and the screens were developed and quantitated using a Fuji BAS 2000 phosphorimager.

Equilibrium Gel Filtration. Equilibrium gel filtration was done as described by Xu et al. (*6*). PRPP binding was determined in reactions containing NAPRTase (0.53 and 2.1 μM), [β-^{32}P]PRPP (0.03−5.4 μM), 1 mM ATP, 7 mM $MgSO_4$, and [^{3}H]glucose in buffer N supplemented with 5 mM DTT. NA binding was assayed in both the presence and absence of 1 mM ATP in reactions containing 150 μM NAPRTase, 100 μM [^{14}C]NA, [^{3}H]glucose, and 5 mM $MgSO_4$ in buffer N supplemented with 5 mM DTT.

Isotope Trapping of [β-^{32}P]PRPP. Isotope trapping (*13*) was performed using [β-^{32}P]PRPP. Binding reactions (50 μL), containing 2 mM ATP, 3.8 μM [β-^{32}P]PRPP (1×10^6 cpm/nmol), 7 mM $MgCl_2$, and 16.6 μM NAPRTase in buffer N supplemented with 5 mM DTT, were preincubated for 5 min. Samples (10 μL) of the binding reaction were injected into 450 μL of the chase buffer (1.5 mM PRPP, 1.0 mM ATP, 7 mM $MgCl_2$, and either 1 mM or 10 μM NA in buffer N supplemented with 5 mM DTT). After 20 s, the reaction was quenched by the addition of 100 μL of 0.5 M EDTA. Samples (10 μL) of the quenched reactions were spotted on PEI−cellulose TLC plates and developed with 0.85 M $NaHPO_4$, pH 3.4 as described previously. For the controls, nonradioactive PRPP was used in the binding reaction, and [β-^{32}P]PRPP was included in the chase buffer.

E−P Hydrolysis. The rate of E-^{32}P hydrolysis was measured in chemical quench experiments in which syringe

A contained 176 μM NAPRTase, 1 mM [γ-^{32}P]ATP (5000 cpm/nmol), 2 mM PRPP, and 7 mM $MgCl_2$ in buffer N supplemented with 5 mM DTT. Syringe B contained 2 mM NA, 20 mM nonradioactive ATP, and 20 mM $MgCl_2$ in buffer N supplemented with 5 mM DTT. Reactions were quenched in 1.0 M NaOH. Portions (140 μL) of the quenched reaction were applied to 1 mL centrifuge columns (*11*) equilibrated in 100 mM NaOH. Column effluents were brought to 1 mL with 100 mM NaOH. Radioactivity was determined by Cerenkov radiation and protein by A_{280} absorbance. The first-order decrease in stoichiometry of phosphorylation vs time was used to calculate the rate constant for E$-^{32}$P hydrolysis.

Product-Stimulated ATPase. The rates of PP_i- and NAMN-stimulated ATPase were investigated at 30 °C using the coupled spectrophotometric assay described by Vinitsky and Grubmeyer (*1*). In the PP_i-stimulated reaction, ATP concentrations of 0.5−9 mM and PP_i concentrations of 25 μM−2.0 mM were used. In the NAMN-stimulated reaction, ATP was fixed at 1 mM and NAMN was varied from 80 μM to 2.5 mM.

Stoichiometry of ATP Usage. The molar stoichoimetry of ATP hydrolyzed to NAMN formed was assayed at various PP_i concentrations. Reactions (1 mL) contained 1.0 mM ATP, 3 mM PEP, 7 mM $MgSO_4$, 5 mM DTT, 0.4 mM NADH, 75 μg/mL pyruvate kinase (PK), 12.5 μg/mL lactate dehydrogenase (LDH), 0−3 mM PP_i, and either 100 μM PRPP and 118 μM [^{14}C]NA or 200 μM PRPP, and 212 μM [^{14}C]NA (500 cpm/nmol) in buffer N. ATP use was monitored continuously as the decrease in A_{340}. At 5, 8, or 10 min, reactions were quenched with 6% perchloric acid, and [^{14}C]NAMN in the quenched samples was separated from substrate [^{14}C]NA by HPLC with the sodium acetate buffer.

RESULTS

ATP Binding and Phosphorylation. ITP is a good alternative substrate for ATP in the coupled NAMN synthesis reaction (V_{max} = 5.1 ± 0.28 units/mg, K_M = 1.16 ± 0.13 mM). As expected for an alternative substrate (*14*), nonradioactive ATP (V_{max} = 3.9 units/mg, K_M = 330 μM) was a competitive inhibitor vs [γ-^{32}P]ITP, giving a K_I of 0.82 ± 0.08 mM (Figure 1).

[γ-^{32}P]ATP rapidly phosphorylates NAPRTase at N1 of His-219, producing a base-stable E−P (*5*). Stoichiometries of phosphorylation typically ranged from 0.8 to 0.9 in the presence of PRPP and from 0.25 to 0.4 in its absence. [In the present work, the extinction coeffient of NAPRTase, determined experimentally using quantitative amino acid analysis, was 1.3-fold higher than the calculated value. Values from Gross et al. (*5*) are corrected here to reflect the revised extinction coefficient for the protein; see Experimental Procedures.] The lower values observed when PRPP was not present likely resulted from ADP binding to E−P, leading to re-formation of ATP. When an ATP regenerating system composed of PEP and pyruvate kinase was added to remove free ADP, stoichiometries of phosphorylation were indistinguishable from those obtained in the presence of PRPP.

Chemical quench techniques were used to follow the rate of enzyme phosphorylation (Figure 2). NAPRTase in one syringe of a chemical quench apparatus was mixed with

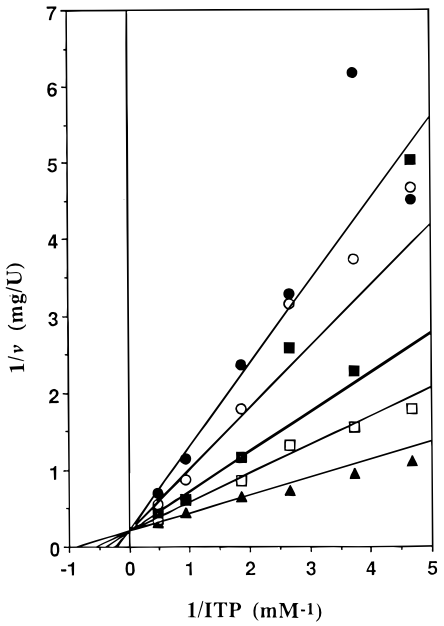

FIGURE 1: Inhibition of [γ-^{32}P]ITP hydrolysis by ATP. Lines represent the simultaneous fit using the program COMPO (*10*); K_I was 0.82 ± 0.07 mM. (▲) no ATP; (□) 0.5 mM ATP; (■) 1.0 mM ATP; (○) 2.0 mM ATP; (●) 3.0 mM ATP.

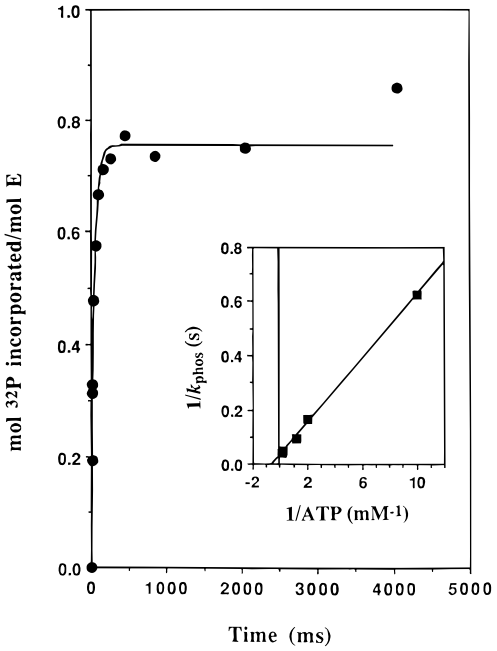

FIGURE 2: Rate of phosphorylation of NAPRTase by [γ-^{32}P]ATP. Chemical quench experiments were performed as described under Experimental Procedures. Data were fit to single-exponential decay equations using linear least-squares regression to obtain k_{phos} at each concentration of [γ-^{32}P]ATP. The experiment shown was conducted at 5 mM [γ-^{32}P]ATP, with the line fit to a k_{phos} of 21.3 s^{-1} and a final stoichiometry of 0.75. (Inset) Double-reciprocal plot of k_{phos} vs [γ-^{32}P]ATP concentration. The maximum rate of phosphorylation, 29.6 ± 1.6 s^{-1}, and $K_{0.5}$, 1.7 ± 0.3 mM, were calculated using HYPER (*10*).

[γ-^{32}P]ATP, pyruvate kinase, and PEP from the second syringe, and then the reaction was quenched in 1 M NaOH, with subsequent determination of E$-^{32}$P. The extent of phosphorylation followed pseudo-first-order kinetics and allowed calculation of the rate constant for NAPRTase phosphorylation (k_{phos}). The k_{phos} values showed a hyperbolic dependence on [γ-^{32}P]ATP concentration, with a maximal

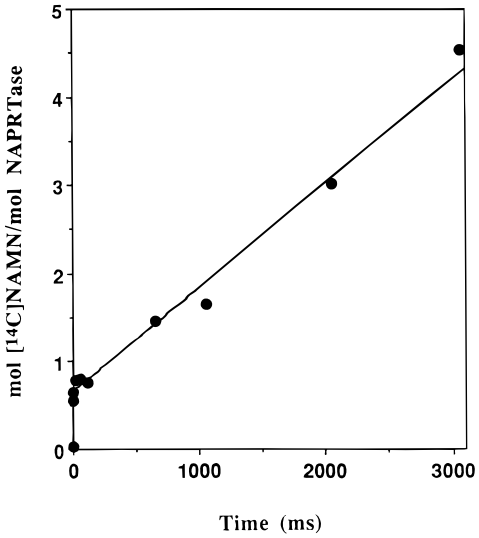

FIGURE 3: Rate of [^{14}C]NAMN formation. Chemical quench experiments were performed as described under Experimental Procedures. [^{14}C]NA in one syringe was added to the preformed E−P·PRPP binary complex in the other. The burst was faster than the resolving time of the equipment and was estimated to be ≥ 500 s^{-1}. The magnitude of the burst was 0.65 mol of [^{14}C]NAMN/mol of NAPRTase and the steady-state rate was 1.2 s^{-1}.

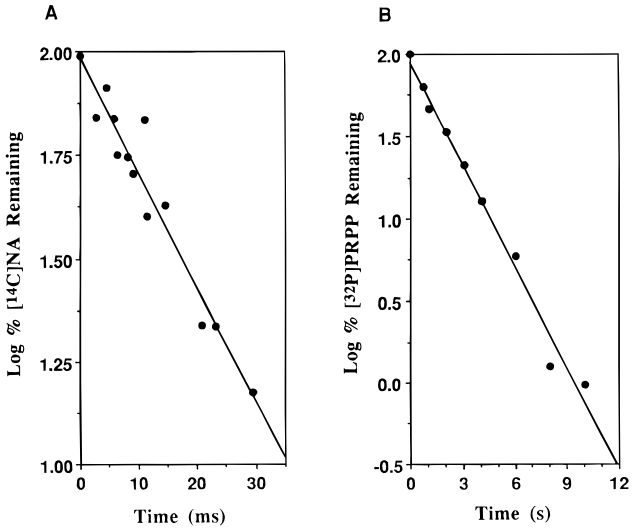

FIGURE 4: Binding of substrates to NAPRTase. Chemical quench experiments were performed as described under Experimental Procedures. (A) A single-turnover experiment with [^{14}C]NA was performed with a molar excess of NAPRTase and allowed calculation of the rate constant for binding, 7.0×10^6 M^{-1} s^{-1}. The experiment shown contained 12.7 μM NAPRTase and 3 μM [^{14}C]-NA. (B) A single-turnover experiment with [β-^{32}P]PRPP was performed with an excess of NAPRTase and allowed calculation of the rate constant for binding, 0.72×10^5 M^{-1} s^{-1}. The experiment shown contained 8.8 μM NAPRTase and 0.33 μM [β-^{32}P]PRPP. Lines in both plots were fit by linear least-squares regression.

value of 29.6 ± 1.6 s^{-1}. The half-maximal rate of enzyme phosphorylation was attained at an ATP concentration ($K_{0.5}$) of 1.7 ± 0.3 mM (Figure 2, inset).

Substrate Binding and Phosphoribosyl Transfer. When NAPRTase, ATP, and PRPP, incubated in one syringe of the chemical quench apparatus, were mixed with [^{14}C]NA from the other syringe and then the reaction was quenched in $HClO_4$, a burst of [^{14}C]NAMN production was observed, followed by steady-state [^{14}C]NAMN formation. The steady-state rate was 1.2 s^{-1} (Figure 3), about half the rate measured at room temperature using the spectrophotometric ATPase assay (k_{cat} = 2.3 s^{-1}). The rate constant for the burst phase was more rapid than the resolving time of our instrument and was estimated to be ≥ 500 s^{-1}. The magnitude of the burst, 0.65 mol of NAMN/mol of NAPRTase, represented approximately 75% of the phosphorylatable NAPRTase molecules measured with the same enzyme preparation.

The very rapid conversion of E−P·PRPP·NA complexes to E−P·NAMN·PP_i allowed the determination of minimal on rates for formation of productive complexes for phosphoribosyl transfer. When [^{14}C]NA in syringe A was mixed with a 10-fold molar excess of NAPRTase, [^{14}C]NAMN formation followed pseudo-first-order kinetics, allowing calculation of the rate constant for the binding of NA to the E−P·PRPP complex as (7.0 ± 0.9) × 10^6 M^{-1} s^{-1} (Figure 4A).

The minimal rate constant for productive PRPP binding to E−P was determined in similar chemical quench experiments in which enzyme was incubated with ATP in one syringe, then mixed with [β-^{32}P]PRPP and NA from the other syringe. The rate constant for PRPP binding to E−P is (0.72 ± 0.04) × 10^5 M^{-1} s^{-1}. This value is close to $k_{cat}/K_{M\ PRPP}$ (0.13×10^6 M^{-1} s^{-1}) measured at 30 °C.

The K_M of MgPRPP in the coupled reaction, 20 μM, is 200-fold lower than the K_M for MgPRPP in the uncoupled reaction and suggests tighter binding of MgPRPP to E−P than to E. To test this, [β-^{32}P]PRPP binding to E−P was

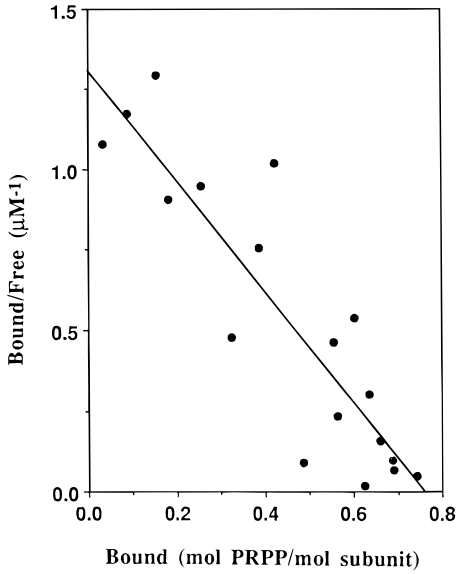

FIGURE 5: Scatchard plot of [β-^{32}P]PRPP binding to E−P. Binding of [β-^{32}P]PRPP to E−P was investigated by equilibrium gel filtration. The values of n and n/f were plotted, allowing calculation of K_d as 0.6 μM with 0.8 binding site/NAPRTase molecule. The line was fit by linear least-squares regression.

determined by equilibrium gel filtration in the presence of 1.0 mM ATP (Figure 5). K_D was 0.59 ± 0.13 μM, with 0.76 ± 0.2 mol of [β-^{32}P]PRPP bound/mol of NAPRTase. The binding of PRPP was also measured in the absence of ATP. In each case, NAPRTase was present at 200 μM and [β-^{32}P]PRPP at 90 μM. With no nucleotide present, the binding stoichiometry was 0.078 mol of [β-^{32}P]PRPP/mol of NAPRTase. The weak binding precluded Scatchard analysis, but assuming 0.8 binding site/enzyme molecule (i.e., the value observed for both PP_i and PRPP binding), K_D was

estimated as 1 mM. When [β-^{32}P]PRPP binding to NAPRTase was assayed in the presence of 5 mM AMP-PCP, 0.036 mol of [β-^{32}P]PRPP/mol of NAPRTase was detected. This value was 25-fold lower than that for [β-^{32}P]PRPP binding to E−P measured in the same experiments (0.88 mol of [β-^{32}P]PRPP/mol of NAPRTase).

NA Binding to E and E−P. Binding of [^{14}C]NA to both the nonphosphorylated and E−P forms of NAPRTase was measured using equilibrium gel filtration in reactions containing 100 μM [^{14}C]NA and 150 μM NAPRTase. When no ATP was present, the binding stoichiometry was 0.045 mol of [^{14}C]NA/mol of NAPRTase, and when 1 mM ATP was included, the stoichiometry was 0.12 mol of [^{14}C]NA/mol of NAPRTase. By assuming an *N* value of 0.8 NA binding site/enzyme molecule, K_D values for the nonphosphorylated and phosphorylated forms of NAPRTase were estimated as 1.7 mM and 0.6 mM, respectively. This weak binding was not studied further.

Isotope Trapping. Isotope trapping was performed to investigate the kinetic competence of the E−P·PRPP binary complex. At the concentrations of NAPRTase (16.6 μM) and [β-^{32}P]PRPP (3.8 μM) used, 96% of the [β-^{32}P]PRPP should be bound to E−P ($K_{D\ PRPP} = 0.6\ \mu$M). In experiments using 1 mM NA in the chase, 93% of the bound [β-^{32}P]-PRPP was converted to [^{32}P]PP$_i$. When 10 μM NA was used in the chase, 87% of the bound [β-^{32}P]PRPP was converted to [^{32}P]PP$_i$. Control experiments showed that the conversion of [β-^{32}P]PRPP to [^{32}P]PP$_i$ was not caused by steady-state turnover in the chase phase of the reaction.

E−P Hydrolysis. When mixed with substrates PRPP and NA, E−^{32}P undergoes complete phosphohydrolysis within the time resolution of experiments done by hand (3 s; *5*). In chemical quench experiments, the decrease in the stoichiometry of E−^{32}P was monitored upon addition of substrates. E−^{32}P·PRPP in one syringe of the chemical quench apparatus was mixed with NA and an excess of nonradioactive ATP from the other syringe. Approximately 90% of the radioactivity initially associated with NAPRTase was lost in 350 ms; however, after 1 s, radioactivity representing 3% of the initial value remained associated with NAPRTase. This radioactivity represents enzyme phosphorylated during steady-state turnover with isotopically diluted [γ-^{32}P]ATP. When the steady-state phosphorylation was subtracted from the hydrolysis data, the rate constant for the first-order loss of E−^{32}P was 6.3 s^{-1} (Figure 6).

NAPRTase Phosphorylation in the Steady State. When NAPRTase reactions containing 3 mM [γ-^{32}P]ATP, 1 mM PRPP, and 1 mM NA were base-quenched from the steady state (1−4 turnovers), the level of E−^{32}P was 0.4 mol of E−P/mol of enzyme. The maximum stoichiometry of phosphorylation in the same experiments was 0.9 (Figure 7). Thus, 44% of the enzyme molecules are phosphorylated during steady-state turnover under V_{max} conditions.

Substrate Inhibition of PP$_i$-Stimulated ATPase. Exogenous PP$_i$ stimulates the ATPase activity of NAPRTase (*1*). The PP$_i$-stimulated ATPase activity of NAPRTase was assayed by the coupled spectrophotometric assay described by Vinitsky and Grubmeyer (*1*) and found to be inhibited at high concentrations of substrate PP$_i$ (Figure 8).

Double-reciprocal plots of v vs ATP were made for each concentration of PP$_i$ tested. These plots were parallel at low concentrations of PP$_i$ and intersected on the ordinate at high concentrations of PP$_i$, results characteristic of ping-pong reactions exhibiting substrate inhibition (*14*). As determined using formulas described by Segel, V_{max} was 5.8 units/mg of NAPRTase, $K_{M\ ATP}$ was 210 μM, $K_{M\ PP_i}$ was 93 μM, and $K_{i\ PP_i}$ was 320 μM.

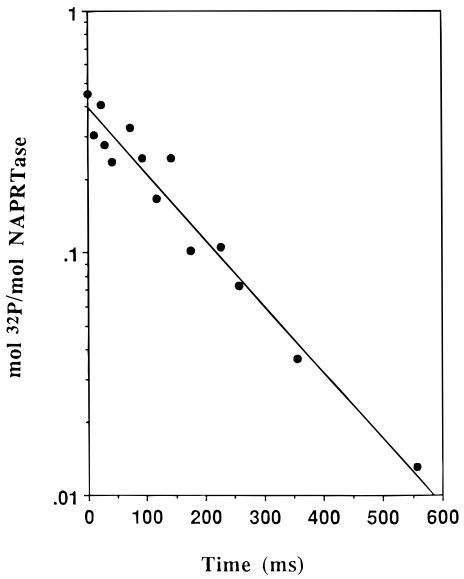

FIGURE 6: Rate of E−^{32}P hydrolysis. Chemical quench experiments were performed as described under Experimental Procedures. The decrease in the stoichiometry of NAPRTase phosphorylation was observed following the addition of substrates PRPP and NA and was used to calculate the rate of E−^{32}P hydrolysis as 6.3 s^{-1}. Data were corrected for steady-state phosphorylation with isotopically diluted [γ-^{32}P]ATP as described in Results.

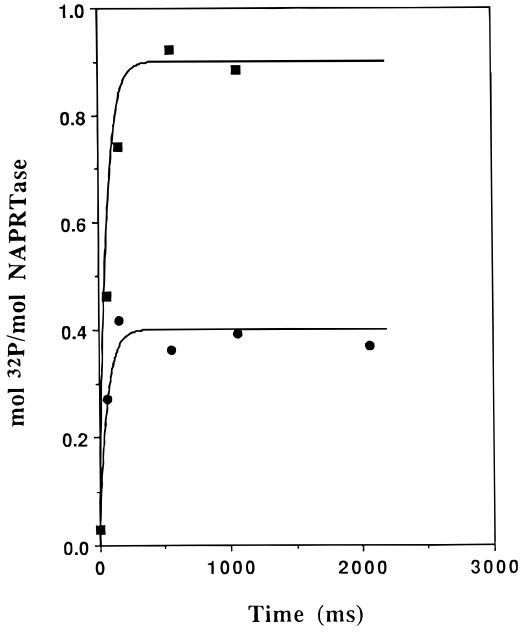

FIGURE 7: NAPRTase phosphorylation during steady-state turnover. The amount (moles) of ^{32}P incorporated per mole of NAPRTase was investigated by mixing enzyme with [γ-^{32}P]ATP and PRPP both with (●) and without (■) NA. Phosphorylation during steady-state turnover was 44% of that detected in the E−^{32}P·PRPP binary complex. The lines represent the equation mol of ^{32}P/mol of E = $\sigma(1 - e^{-k_{phos}t})$, where σ is the final stoichiometry, k_{phos} (29 s^{-1}) is the rate constant for NAPRTase phosphorylation, and t is the time in seconds. The value of σ was 0.4 (●) and 0.9 (■).

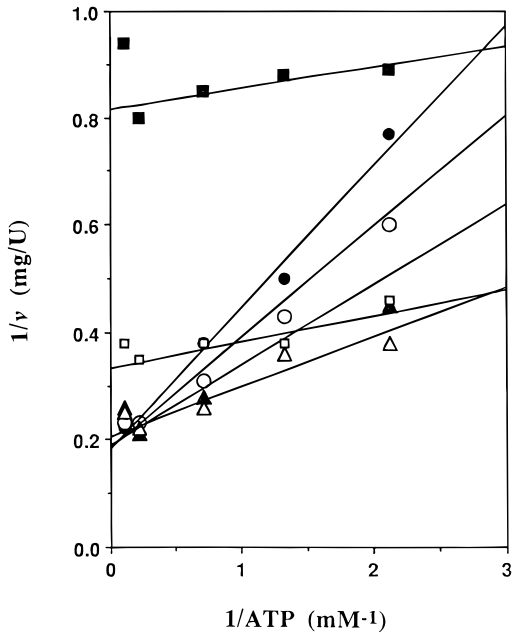

FIGURE 8: Double-reciprocal plot of PP_i-stimulated ATPase activity vs ATP concentration at (■) 25 μM PP_i; (□) 100 μM PP_i; (△) 500 μM PP_i; (▲) 1 mM PP_i; (○) 1.5 mM PP_i; and (●) 2 mM PP_i. The $K_{I\ PP_i}$, $K_{M\ PP_i}$, $K_{M\ ATP}$, and V_{max} values were 320 μM, 93 μM, 210 μM, and 5.8 units/mg, respectively. The lines represent a simultaneous fit to the equation for substrate inhibition described by Segel (*14*).

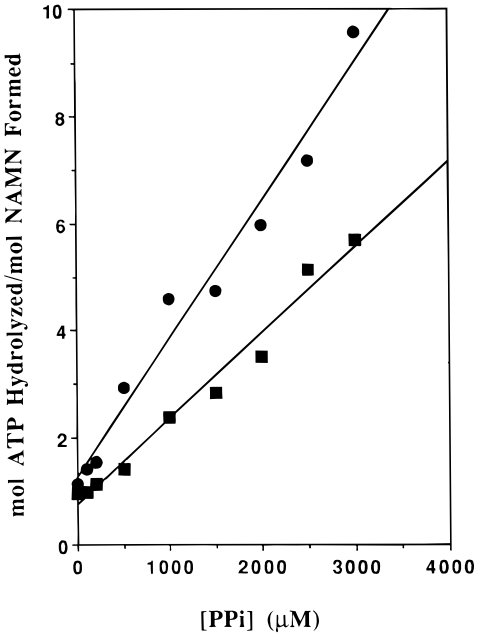

FIGURE 9: Comparison of ATPase and NAMN synthesis activities of NAPRTase at increasing concentrations of PP_i. [^{14}C]NA and PRPP concentrations were both fixed at 100 (●) and 200 μM (■). Lines represent linear least-squares fits to the individual data sets.

NAMN-Stimulated ATPase. As mentioned in the preceding paper (*17*), an NAMN-stimulated ATPase activity was detected using the coupled spectrophotometric assay (*1*). We found that the reaction rate demonstrated hyperbolic dependence on NAMN concentration, with no detectable substrate inhibition. The program HYPER (*10*) was used to solve for $K_{M\ NAMN}$ (620 ± 50 μM) and V_{max} (0.88 ± 0.03 unit/mg).

Stoichiometry of ATP Usage. When the concentrations of [^{14}C]NA and PRPP were fixed at 100 or 200 μM (Experimantal Procedures), the stoichiometry of ATP use increased in a linear fashon with increasing PP_i concentration (Figure 9). The slopes were inversely proportional to PRPP (and NA) concentration.

NAMN Synthesis from Nonphosphorylated NAPRTase. Phosphoribosyl transfer chemistry was fast when initiated by the addition of [^{14}C]NA to E−P·PRPP (Figure 3). To determine if there were any slow steps in the mechanism between binding of the first substrate, MgATP, and phosphoribosyl transfer, chemical quench experiments were performed in which apoenzyme in one syringe was mixed with [^{14}C]NA, PRPP, and ATP in the other. A rapid burst of [^{14}C]NAMN formation was observed with $n = 0.8$, $k_{obs} = 15\ s^{-1}$, and a steady-state turnover of $0.8\ s^{-1}$ (data not shown).

Table 1: Rate Constants for NAPRTase

constant	value	comments
k_1	$2 \times 10^4\ M^{-1}\ s^{-1}$	$k_{cat}/K_{0.5}$; determined in pre-steady-state phosphorylation studies
k_{-1}	$16\ s^{-1}$	$K_I \times k_1$
k_2	$29\ s^{-1}$	determined from pre-steady-state phosphorylation studies
k_{-2}	$\geq 3.5\ s^{-1}$	$k_{exchange}$; ATP/ADP exchange reaction
k_3	$\geq 30\ s^{-1}$	calculated from pre-steady-state NAMN formation
k_{-3}	$5 \times 10^3\ M^{-1}\ s^{-1}$	$k_{exchange}/K_{M\ ADP}$; ATP/ADP exchange reaction
k_4	$0.72 \times 10^5\ M^{-1}\ s^{-1}$	experimentally determined
k_{-4}	$0.04\ s^{-1}$	$K_{D\ PRPP} \times k_4$
k_5	$7.0 \times 10^6\ M^{-1}\ s^{-1}$	experimentally determined
k_{-5}		
k_6	$\geq 500\ s^{-1}$	pre-steady-state formation of NAMN
k_{-6}		
k_7	$6.3\ s^{-1}$	determined from E-^{32}P hydrolysis
k_{-7}		
k_8	$5.2\ s^{-1}$	calculated from steady-state phosphorylation
k_{-8}		

DISCUSSION

The work presented in this and the accompanying paper (*17*) allows a more complete description of the structural and kinetic features of energy coupling in NAPRTase. Here, we first discuss the kinetic mechanism in segments corresponding to ATP use, NAMN formation, and product release. Rate constants for this segment of the mechanism are summarized in Table 1 and Scheme 2. We then discuss the side reactions catalyzed by the enzyme. Finally, we show how NAPRTase utilizes the differential properties of E and E−P forms to couple ATP hydrolysis to NAMN synthesis and demonstrate that this mechanism results in a coupling that is intrinsically inefficient.

ATP Use. The use of ATP involves four nominal steps: nucleotide binding, phosphorylation of His-219, release of ADP, and a change in the active site of the enzyme that allows high-affinity PRPP binding. The alkaline stability of E−P provided a means to measure the extent of phosphorylation in the pre-steady state using chemical quench techniques. The rate constant for covalent enzyme phosphorylation from E·ATP was measured at $29\ s^{-1}$. The $k_{cat}/K_{0.5}$ for MgATP in phosphorylation of NAPRTase ($2 \times 10^4\ M^{-1}\ s^{-1}$) provides a minimum estimate of the rate constant

Scheme 2

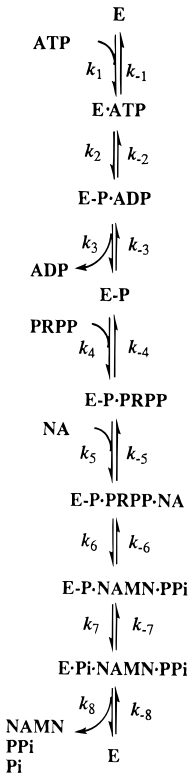

for ATP binding and is supported by k_{cat}/K_M (5×10^3 M^{-1} s^{-1}) in the overall reaction. These rates are slow compared to rate constants for ATP binding in other enzymes, typically about 10^6 M^{-1} s^{-1} (*15*, *16*).

Calculation of the rate of ADP dissociation depends on the assumption that this step is compulsory before binding of PRPP and NA, as demonstrated by Hanna et al. (*4*), and is not an independent event, as originally proposed by Kosaka et al. (*3*). This conclusion is also supported by the apparent competion between ligands noted in the previous paper (*17*). Since the rate of ATP-coupled NAMN formation from unliganded NAPRTase occurs at 15 s^{-1}, close to the rate of E−P formation of 29 s^{-1}, ADP release must be relatively rapid, at least 30 s^{-1}. Rapid ADP release is also consistent with the observation that ADP/ATP isotope exchanges in the absence of PRPP and NA are consistently faster than the rate of net forward catalysis (*1*, *3*, *18*). Following the same logic used to consider ADP release, the conformational change associated with high-affinity PRPP and NA binding must also proceed at a rate of at least 30 s^{-1}.

NAMN Formation. At high levels of NA and PRPP, the rate of NAMN formation from preformed E−P complexes was at least 500 s^{-1}, faster than other steps in the mechanism. The amplitude of the burst of NAMN formed was approximately the same as the amount of E−P and indicated that all phosphorylated sites were capable of NAMN formation. Rapid on-enzyme phosphoribosyl transfer chemistry appears to be a feature of several of the PRTases, including HGPRTase, in which the phosphoribosyl transfer rate of 131 s^{-1} is 19-fold faster than net forward IMP formation (*6*), and OPRTase, in which a transfer rate of 300 s^{-1} is 5-fold faster than net catalysis (this laboratory, unpublished results). Because of the phosphohydrolytic stability of E−P·PRPP complexes, it was possible to measure the K_D of MgPRPP of 0.6 μM, which compares to the value of 1.3 μM for HGPRTase (*6*). The measured rate constant for PRPP binding (0.72×10^5 M^{-1} s^{-1}) was consistent with values measured for HGPRTase (1×10^5 M^{-1} s^{-1}; *6*). The k_{on} and K_D for PRPP allow calculation of an off rate of 0.04 s^{-1}, suggesting that E−P·PRPP complexes are stable on the catalytic time scale. Isotope trapping showed that these complexes were catalytically productive and verified that the off rate for PRPP was not significant compared to the rate of forward catalysis.

The K_D values for the weak equilibrium NA binding to E and E−P (1.7 and 0.6 mM) are far higher than the K_M of 1.5 μM in the coupled reaction and are consistent with the conclusion from steady-state kinetics (*4*) that PRPP binding precedes binding of NA in a compulsory ordered fashion. The rate constant for NA binding to E−P·PRPP, 7.0×10^6 M^{-1} s^{-1}, is similar to that for base binding to HGPRTase (*6*).

E−P Hydrolysis and Product Release. The maximal rate for hydrolysis of preformed E−P complexes when mixed with PRPP and NA, 6.3 s^{-1}, was far slower than the rate of NAMN formation by the same complexes, 500 s^{-1}. This difference demonstrates that NAMN formation precedes E−P hydrolysis and that E−P hydrolysis is a participant in determining the overall rate constant for forward net catalysis of 2.3 s^{-1} at 22−23 °C. Employing the formula $1/k_{cat} = 1/k_1 + 1/k_2 + ... + 1/k_n$, where k_n are net rate constants (*19*) for steps in forward catalysis, and using the measured values for enzyme phosphorylation (29 s^{-1}), phosphoribosyl transfer (500 s^{-1}), and E−P hydrolysis (6.3 s^{-1}) gives a value of 5.1 s^{-1} for k_{cat} and suggests that at least one other step, with a rate of 4.5 s^{-1}, must also participate in rate limitation. Since rate constants were measured for all steps up to formation of E·P_i·NAMN·PP_i, the missing slow step must be subsequent to E−P hydrolysis. The proportion of active enzyme phosphorylated in the steady state at V_{max}, 0.44, shows that slightly less than half the enzyme is in complexes that have not yet undergone E−P hydrolysis, with the remainder in complexes in which E−P has been hydrolyzed. These proportions, combined with previously determined net rates, independently show that steps following E−P hydrolysis and preceding regeneration of active apoenzyme have a net rate constant of about 5.2 s^{-1}. It is not yet clear whether product release steps, or conformational changes that regenerate active apoenzyme, contribute to the rate limitation.

Alternative Reactions Catalyzed by NAPRTase. NAPRTase catalyzes rapid PP_i-stimulated and NAMN-stimulated ATPase reactions and a slow and reversible ATP-uncoupled NAMN formation reaction. The alternative reactions provide information valuable to a consideration of coupling.

The PP_i-stimulated ATPase involves binding of ATP and phosphoryl transfer to form E−P, binding of PP_i, followed by E−P hydrolysis and product release. The maximal rate (4.4 s^{-1}, at 30 °C) and $K_{M\ ATP}$ (0.21 mM) for this reaction suggest that steps which contribute to rate limitation are similar to those for overall catalysis (2.8 s^{-1} at 30 °C, $K_{M\ ATP}$ 0.3 mM). The K_M for PP_i was 93 μM. The existence of substrate inhibition by PP_i ($K_I = 320$ μM) suggested that binding of PP_i to E could occur and prevent ATP binding. PP_i binding to E was detected (*17*), with a K_D of 140 μM, and n values (0.8 mol/mol of NAPRTase) similar to those for enzyme phosphorylation. NAMN-stimulated ATPase

Scheme 3

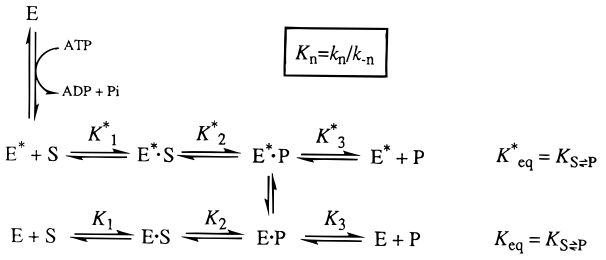

was slower, 0.67 s^{-1}, and did not show substrate inhibition by NAMN. Uncoupled NAMN synthesis occurs with a $K_{M\ PRPP}$ of 4.5 mM, a $K_{M\ NA}$ of 0.3 mM, and a V_{max} of 0.29 unit/mg of NAPRTase (*1*).

Stoichiometry of ATP Use. Several groups have shown a 1:1 molar stoichiometry of ATP hydrolyzed per NAMN formed when assays are performed under initial rate conditions (*1*, *20*−*22*). The mechanism of Scheme 1 suggests that stoichiometry will rise as product accumulates. When PP_i is allowed to accumulate, ATP use by NAPRTase no longer follows unit stoichiometry with NAMN formation, as it does under initial velocity conditions, but instead rises in linear proportion to PP_i concentration. Stoichiometries as high as 10 mol of ATP hydrolyzed/mol of NAMN formed were observed, and no apparent limit on this value could be discerned or predicted.

Energy Coupling by NAPRTase. To understand energy coupling by NAPRTase, three observations must be explained. First, the ATP usage in the reaction follows variable stoichiometry, rising as [PP_i] increases. Second, the high product-to-substrate ratios achieved by NAPRTase are a feature of the steady state and not an equilibrium property. Finally, the product-to-substrate ratio for NAMN synthesis ([NAMN][PP_i]/[PRPP][NA]) increases 1500-fold when ATP is present and being hydrolyzed. This value, although quite substantial, is far below the value of 1.4×10^6 expected for an ATP-driven reaction under these conditions (*23*). These three phenomena, each of which represents a type of energetic inefficiency, have different origins and their analysis suggests fundamental intrinsic inefficiency in the ability of ATP to drive solution-phase coupled reactions through conformational intermediates.

For many ATP-driven reactions it is suggested that ATP hydrolysis drives a series of conformational changes that selectively alter the affinity of enzyme for substrates and products. Jencks (*24*, *25*) has also shown that as long as the constituent steps of ATP hydrolysis and a second process are intertwined, and the intermediates obey "rules" that prevent their unproductive decomposition, the two processes must be energetically coupled. While these precepts are logical and attractive, a brief theoretical analysis for a one-substrate one-product reaction shows that the enzyme properties required to carry out such a reaction may be difficult to achieve. Scheme 3 considers the ATP-driven interconversion of S and P. In this scheme, the equilibrium constants K_n are each defined as k_n/k_{-n}. To separate the chemistry of ATP use from the basic problem of energy coupling, ATP hydrolysis is used to convert a relaxed form of the enzyme, E, to an energized form, E*, before any steps of the S to P conversion. Complete reaction cycles are shown for S ⇌ P catalysis by both the E (lower horizontal equation) and E* (upper horizontal equation) forms of the enzyme. For each independent horizontal equation, K_{eq} is that for the conversion of S ⇌ P, $K_{S\rightleftharpoons P}$. The ATP-coupled pathway starts in the upper left with E, which after ATP use is converted to E* and proceeds by binding S and then chemical catalysis to E*·P, which then forms E·P, followed by product release to re-form E. If the coupled pathway followed only these productive steps, $K_{eq} = K_{S\rightleftharpoons P}(K_{hydr\ ATP})$, where $K_{hydr\ ATP}$ is K_{eq} for the hydrolysis of ATP to ADP and P_i.

Scheme 3 makes it possible to consider the binding properties of the two enzyme forms that would favor the coupled pathway. The ideal binding behavior for E* is high affinity for substrate, allowing it to bind S from low S concentrations. However, since the K_{eq} for each horizontal equation is $K_{S\rightleftharpoons P}$ and is the product of the K values for its constituent steps, tight binding of S by E* (a large value for K_1*) also demands either a compensatory tight binding of P (a small K_3*) or a poor equilibrium for the internal complexes (a small K_2*). In the former case, as [P] increases, inhibitory E*·P complexes will be formed, stopping the forward reaction. For the E form of the enzyme, a relatively low affinity for product would allow P to be released against a high P concentration. Again, however, constraints placed on this binding behavior by K_{eq} mean that binding of S by E must also be poor. Therefore, in terms of binding affinities, it appears most likely that E* will bind both S and P tightly and that E will bind both P and S loosely. The tight binding of P to E* leads to severe product inhibition.

The relaxation of the E* form of the enzyme to the E form is the final step of the ATP hydrolysis and must be linked to P formation if energy is to be conserved. Thus, only E*·P and not E* and E*·S complexes can be allowed to decompose to E. Scheme 3 thus demands an intrinsic signal for linking P formation with deenergization of E*. That trigger is the presence of P in the active site of E*. Since E*·P complexes can be formed by the binding of adventitious P to newly formed E*, the compulsory relaxation of E*·P to E ·P provides a way to discharge adventitiously bound P. This discharge obviates the product inhibition caused by the tight P binding demanded of E* but comes at an energetic cost, the net hydrolysis of one molecule of ATP.

In addition, as Scheme 3 is written, E·P, an intermediate on the coupled pathway, can convert to E·S to release S, a pathway that also leads to net unproductive ATP hydrolysis. This pathway is formally necessary, but its practical significance will depend on the rate of the E·P to E·S conversion.

Scheme 3 leads to energetic inefficiency that is exactly analogous to the three observations made with NAPRTase at the start of this section. First, because adventitious P binding to E* will increase as [P] increases and because this binding leads to net ATP hydrolysis, the stoichiometry of ATP use will also increase as product accumulates. At any point in the reaction, the instantaneous stoichiometry is a function of the E* relaxation induced by P and that induced by S:

$$\text{moles of ATP consumed/moles of P formed} = 1 + (k^*_{-3}[P]/k^*_1[S])$$

Second, the scheme is fundamentally steady state in its nature: When ATP is exhausted, the P-stimulated relaxation

of E* will immediately consume any E* arising from the overall reverse reaction, at $v = V_{max}[P]/([P] + K_{M\ P})$, where V_{max} is the rate for P-stimulated decomposition of E*. Finally, the scheme is fundamentally inefficient because of the ability of E·P formed from E*·P to revert to E·S and thus E + S without re-formation of ATP. The partitioning of E·P between the productive and unproductive fates is the ratio of the dissociation rate of P from E·P (k_3) to the net rate (*19*) for its conversion to E + S, $k_{-2}[k_{-1}/(k_{-1} + k_2)]$

$$\text{partition ratio} = k_3/[k_3 + k_{-2}\{k_{-1}/(k_{-1} + k_2)\}]$$

Each of these three sources of inefficiency can be minimized by a change in the properties of the enzyme. If $k^*_{\pm 3}$ were reduced, then the product-stimulated decomposition of E* would be lessened, reducing two sources of energetic inefficiency. To eliminate the binding of P to E* would require the total occlusion of the active site from solvent, so that P could neither bind to E* nor leave E*·P, although S must be able to bind freely. Such occluded states are proposed by Jencks (*24*) and Krupka (*26*) in their analyses of transporters. The movement of a peptide loop to cover the active site, as suggested for other PRTases (*27*, *28*), would effectively occlude the active site from all ligands, but the effect would not discriminate S and P. It is difficult in practical terms to envision how such an occluded state could occur in an enzyme operating in solution. Therefore, it seems that adventitious P binding is unavoidable and will doom ATP-coupled enzymes to inefficiency.

To eliminate the third source of inefficiency, k_{-2} must be effectively zero. Essentially this behavior would mean that E and E* differ greatly in their catalytic ability. The ability of ATP sulfurylase to drive a 5.4×10^6-fold change in the K_{eq} for the forward reaction (*29*) suggests that the rate of the uncoupled reverse reaction is minimal in that case, although the high stoichiometry of GTP use shows that other sources of inefficiency have not been eliminated.

The properties of Scheme 3 can be broadly extrapolated to NAPRTase, although its complexity with three substrates and four products makes this difficult. In NAPRTase, alternation occurs between two enzyme forms, E and E−P, with E·P_i complexes assumed to have the same properties as E. The two forms show dramatic differences in their binding and catalytic properties. Previously, evidence for a cycle of affinity changes came from the 200-fold differences in K_M values for MgPRPP (22 μM vs 4.5 mM) and NA (1.5 μM vs 0.29 mM) in the presence and absence of ATP. The present work showed that productive binding of MgPRPP to E−P (K_D of 0.6 μM) was about 2000-fold tighter than the binding to apoenzyme (estimated K_D of 1 mM; *17*). Binding of NA directly to E or E−P was poor, in keeping with the required kinetic order of the reaction. Interaction with reaction products was less clearly affected by the phosphorylation state. The K_D for binding of product PP_i to E was measured at 140 μM, and binding to phosphoenzyme can be estimated from its K_M in the PP_i-stimulated ATPase reaction, 93 μM. The K_D for binding of NAMN to E−P is estimated at 620 μM from the K_M for the NAMN-stimulated ATPase. No K_D values are known for binding of P_i to the enzyme.

In its catalytic rate, E−P is also enhanced over E. The k_{cat} in the forward uncoupled reaction, 0.3 s^{-1}, is about 1500-fold slower than the value of 500 s^{-1} determined for the on-enzyme formation of NAMN by E−P at 22 °C. If the conversion is assumed to proceed through a single transition state, then the presence of the phosphoryl group lowers that barrier by about 4.3 kcal/mol, about the same as the amount of energy represented in the ATP-driven gradient of products over substrates.

The variation of ATP stoichiometry as the PP_i concentration increases arises from the necessity for a linkage between steps of ATP use and NAMN synthesis. NAPRTase clearly uses PP_i to signal that the active site contains products and that the high-affinity E−P state can collapse to the low-affinity E·P_i. As PP_i builds up in the medium, this signal molecule can bind adventiously, causing E−P hydrolysis (PP_i-stimulated ATPase). Thus, NAPRTase phosphoenzyme has become discriminatory toward substrate (PRPP) and product (PP_i) molecules: When PRPP is bound, E−P is stable and undergoes forward reaction, and when PP_i is bound, E−P decomposes, expelling PP_i and allowing the cycle to start again. The alternative fates for E−P cause a PP_i-dependent variation in the stoichiometry of ATP hydrolyzed per NAMN made but allow the enzyme to make NAMN even in the presence of product/substrate ratios well above K_{eq}.

ACKNOWLEDGMENT

We thank Mr. Yiming Xu for many helpful and patient discussions.

REFERENCES

1. Vinitsky, A., and Grubmeyer, C. T. (1993) *J. Biol. Chem. 268*, 26004−26010.
2. Rajavel, M., Gross, J., Segura, E., Moore, W. T., and Grubmeyer, C. (1996) *Biochemistry 35*, 3909−3916.
3. Kosaka, A., Spivey, H. O., and Gholson, R. K. (1977) *Arch. Biochem. Biophys. 179*, 334−341.
4. Hanna, L. S., Hess, S. L., and Sloan, D. L. (1983) *J. Biol. Chem. 258*, 9745−9754.
5. Gross, J., Rajavel, M., Segura, E., and Grubmeyer, C. (1996) *Biochemistry 35*, 3917−3924.
6. Xu, Y., Eads, J., Sacchettini, J. C., and Grubmeyer, C. (1997) *Biochemistry 36*, 3700−3712.
7. Grubmeyer, C., and Penefsky, H. S. (1981) *J. Biol. Chem. 256*, 3718−3727.
8. Ebert, R. F. (1986) *Anal. Biochem. 154*, 431−435.
9. Vinitsky, A., Teng, H., and Grubmeyer, C. T. (1991) *J. Bacteriol. 173*, 536−540.
10. Cleland, W. W. (1979) *Methods Enzymol. 63*, 103−139.
11. Penefsky, H. S. (1977) *J. Biol. Chem. 252*, 2891−2899.
12. Jensen, K. F., Houlberg, U., and Nygaard, P. (1979) *Anal. Biochem. 98*, 254−263.
13. Rose, I. A. (1980) *Methods Enzymol. 64*, 47−59.
14. Segel, I. H. (1975) *Enzyme Kinetics*, pp 826−830, John Wiley and Sons, New York.
15. Hanel, A. M., and Jencks, W. P. (1990) *Biochemistry 29*, 5210−5220.
16. Holzbaur, E. L., and Johnson, K. A. (1989) *Biochemistry 28*, 5577−5585.
17. Rajavel, M., Lalo, D., Gross, J. W., and Grubmeyer, C. (1998) *Biochemistry 37*, 4181−4188.
18. Kosaka, A., Spivey, H. O., and Gholson, R. K. (1971) *J. Biol. Chem. 246*, 3277−3283.
19. Cleland, W. W. (1975) *Biochemistry 14*, 3220−3224.
20. Honjo, T., Nakamura, S., Nishizuka, Y., and Hayaishi, O. (1966) *Biochem. Biophys. Res. Commun. 25*, 199−204.
21. Smith, L. D., and Gholson, R. K. (1969) *J. Biol. Chem. 244*, 68−71.

22. Niedel, J., and Dietrich, L. S. (1973) *J. Biol. Chem. 248*, 3500−3505.
23. Rosing, J., and Slater, E. C. (1972) *Biochim. Biophys. Acta 267*, 275−290.
24. Jencks, W. P. (1980) *Adv. Enzymol. 51*, 75−106.
25. Jencks, W. P. (1989) *J. Biol. Chem. 264*, 18855−18858.
26. Krupka, R. M. (1993) *Biochim. Biophys. Acta 1183*, 114−122.
27. Scapin, G., Ozturk, D., Grubmeyer, C., and Sacchettini, J. C. (1995) *Biochemistry 34*, 10744−10754.
28. Henriksen, A., Aghajari, N., Jensen, K. F., and Gajhede, M. (1996) *Biochemistry 35*, 3803−3809.
29. Liu, C., Suo, Y., and Leyh, T. S. (1994) *Biochemistry 33*, 7309−7314.

BI972014W